Effects of Non-Linear Suspension on Hunting and Critical Velocity of Railway Wheelset

A. Karami Mohammadi*
Department of Mechanical Engineering,
Shahrood University of Technology, Shahrood, Iran
E-mail: akaramim@yahoo.com
*Corresponding author

N. Ale Ali
Department of Mechanical Engineering,
Shahrood University of Technology, Shahrood, Iran
E-mail: n_aleali@yahoo.com

Received: 16 April 2012, Revised: 18 December 2012, Accepted: 27 April 2013

Abstract: In this paper, effects of non-linear suspension on dynamic behavior of a railway wheelset have been studied. Nonlinear dynamic model of wheelset motion has been derived. Four coordinates are used and two constrains have been found, therefore, two degrees of freedom are remained. Contact forces between the wheels and rails have been calculated using Vermeulen-Johnson theory. Constant creep coefficients have been taken into consideration. Lateral suspension is dry friction which has been modeled by using Kolesch theory. Runge-kutta method has been used for solving the equations and results are presented to obtain limit cycles due to hunting behavior of the wheelset.

Keywords: Critical Velocity, Hunting, Limit Cycle, Railway Wheelset

Reference: Karami Mohammadi, A., and Ale ali, N., "Effects of non-linear suspension on hunting and critical velocity of railway wheelset", Int J of Advanced Design and Manufacturing Technology, Vol. 6/ No. 2, 2013, pp. 51-59..

Biographical notes: A. Karami Mohammadi received his BSc degree in Mechanical engineering from Sharif University of Technology and his MSc and PhD in Mechanical Engineering from Amirkabir University of Technology in Tehran, Iran. Since 1986 he has involved in researches related to the vehicle industries. Since 1988 he is assistant professor in the Department of Mechanical Engineering of Shahrood University of Iran. **N. Ale Ali** received his BSc degree in Railway engineering from Iran University of Science Technology and his MSc in Mechanical Engineering from Shahrood University of Technology, Iran. At present he is a PhD student at the Department of Mechanical Engineering of Shahrood University of Iran.

1 INTRODUCTION

The wheelset motion is considered to be stable if for a slight lateral displacement or yaw angle the wheelset moves back to its central position after a damped oscillatory parasitic motion. Instability occurs if for some small irregularities an excited vibration takes place, so that the maximum amplitudes increase and the parasitic motion is finally restricted by flange contact. This motion is known as hunting, a common mode of instability in rail vehicles, which is a significant hindrance to high speed rail vehicle operations.

The hunting phenomenon begins as a self excited lateral yaw oscillation of the wheelset when the vehicle speed surpasses a certain critical speed. Therefore, the term critical speed as used in this paper, refers to the speed of the vehicle beyond which hunting appears as an undamped motion of the wheelset constrained by the wheel flange and the rail.

A history of vehicle stability implies a retrospective view on 150 or even 200 years [1]. The kinematic motion of a single wheelset with conical profiles has been well understood at least since Stephenson [2]. H. True et al, investigated Cooperrider's mathematical model of a railway bogie running on a straight track due to its interesting nonlinear dynamics [3]. In their article a detailed numerical investigation was made of the dynamics in a speed range, where many solutions existed, but only a couple of which were stable. M. Ahmadian and S. Yang presented an analytical investigation of Hopf bifurcation and hunting behavior of a rail wheelset with nonlinear primary yaw dampers and wheel-rail contact forces [4]. They demonstrated that the nonlinearities in the primary suspension and flange contact contribute significantly to the hunting behavior, and both the critical speed and the nature of bifurcation are affected by the nonlinear elements.

H. Yabuno et al, shown by using the center manifold theory and the method of normal form, that the nonlinear characteristics of the bifurcation in a wheelset model with two degrees of freedom are governed by a single parameter, hence each nonlinear force need not to be detected when examining the nonlinear characteristics [5]. Also, they proposed a method of determining the governing parameter from experimentally observed radiuses of the unstable limit cycle. Next, they experimentally investigated the variation of the parameter due to the presence of linear spring suspensions in the lateral direction and discuss the variation of the nonlinear characteristics of the hunting motion, which depends on the lateral stiffness.

In this paper, effects of non-linear suspension on dynamic behavior of a railway wheelset have been studied. Nonlinear dynamic model of wheelset motion has been derived. Four coordinates are used and two constrains have been found, therefore, two degrees of freedom are remained. Contact forces between the wheels and rails have been calculated using Vermeulen-Johnson theory. Constant creep coefficients have been taken into consideration. Lateral suspension is dry friction which has been modeled by using Kolesch theory. Runge-kutta method has been used for solving the equations and results are presented to obtain limit cycles due to hunting behavior of the wheelset.

2 MODELING

According to Figure 1, four coordinates, vertical (z) and lateral (y) motions, and yaw (ψ) and roll (φ) rotations are considered. XYZ is a fixed coordinate system, and xyz and $x'y'z'$ are body coordinate systems. $x'y'z'$ coordinate is introduced due to rotation of yaw around *Z* axis, and xyz coordinate are due to the rotation of roll around *x* axis. In this condition, transformation matrix is:

$$\begin{bmatrix} X \\ Y \\ Z \end{bmatrix} = \begin{bmatrix} \cos\psi & -\cos\varphi\sin\psi & \sin\psi\sin\varphi \\ \sin\psi & \cos\psi\cos\varphi & -\sin\varphi\cos\psi \\ 0 & \sin\varphi & \cos\varphi \end{bmatrix} \begin{bmatrix} x \\ y \\ z \end{bmatrix} \quad (1)$$

There are also two coordinates to define the contacts of wheelset that are shown in Figure 2. The left and right contact forces are defined in the left and right contact coordinates respectively, and the parameters defined in these coordinates are demonstrated by subscripts *cl* and *cr,* respectively. It should be noticed that wheelset moves in straight line with constant velocity *V* and contact surface between wheel and rail is assumed to be a point contact.

Details of this contact points are shown in Figure 2. Wheel moves with constant velocity, so speed of rotation of its pitch rotation is constant. Thus angular velocity of wheelset can be shown as three rotational velocities.

$$\vec{\omega}_1 = \dot{\psi}\,\hat{\mathrm{K}}\ , \qquad \vec{\omega}_2 = \dot{\varphi}\,\hat{\mathrm{i}}\ , \qquad \vec{\omega}_3 = \frac{V}{r_c}\hat{\mathrm{j}} \quad (2)$$

Therefore, the total angular velocity of the wheelset in the body wheelset coordinate is defined as :

$$\vec{\omega} = \vec{\omega}_1 + \vec{\omega}_2 + \vec{\omega}_3 = \dot{\phi}\,\hat{\mathrm{i}} + \left(\dot{\psi}\sin\phi + \frac{V}{r_c}\right)\hat{\mathrm{j}} + \dot{\psi}\cos\phi\,\hat{\mathrm{k}} \quad (3)$$

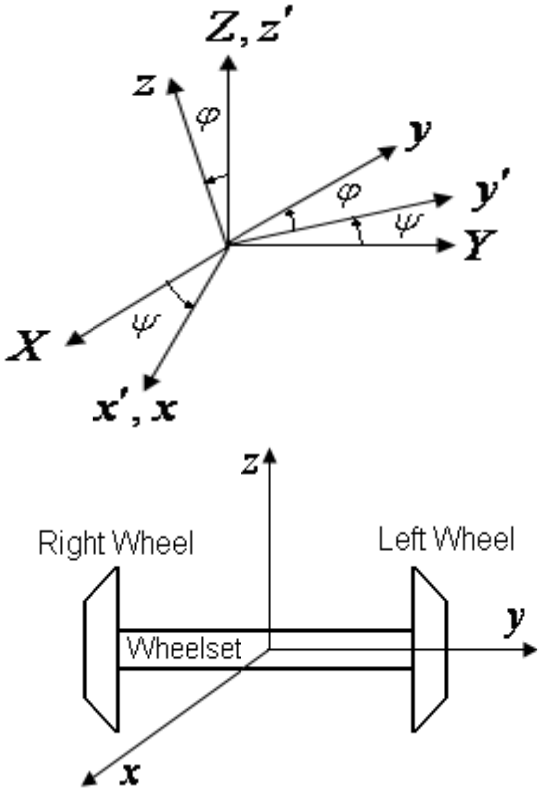

Fig. 1 Different Coordinates for explanation of wheelset movement

According to Figure 2, two constraints can be defined for this motion. The first constraint has defined according to Figure 3, as:

$$\sin\varphi = \frac{|r_{clz}| - |r_{crz}|}{L} \tag{4}$$

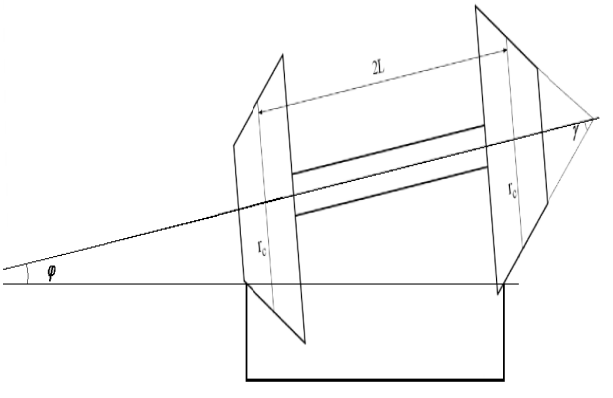

Fig. 2 Position of wheel set on the rail

The second constraint is obtained by defining five vectors (Figure 4). In these vectors, r_1 is distance between centre of track and contact point, r_2 is the displacement distance on the surface of wheel S due to movement of wheelset and vector r_3 is distance between contact point and central of wheelset axel. Vector r_G represents the centre of gravity of wheelset and vector r_4 is defined between end of r_3 and centre of gravity of wheelset. These vectors are defined in $x'y'z'$ coordinate.

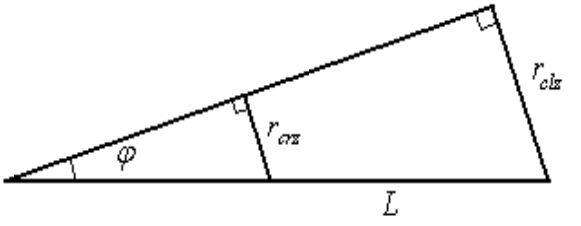

Fig. 3 Roll constrain for wheelset's movement

$$\begin{aligned}
\vec{r}_1 &= L\,\hat{\mathrm{j}}' \\
\vec{r}_2 &= S\left(\cos(\varphi+\gamma)\,\hat{\mathrm{j}}' + \sin(\varphi+\gamma)\,\hat{\mathrm{k}}'\right) \\
\vec{r}_3 &= r_c\left(-\sin\varphi\,\hat{\mathrm{j}}' + \cos\varphi\,\hat{\mathrm{k}}'\right) \\
\vec{r}_4 &= L\left(-\cos\varphi\,\hat{\mathrm{j}}' - \sin\varphi\,\hat{\mathrm{k}}'\right) \\
\vec{r}_G &= y'\hat{\mathrm{j}}' + (z' + r_c)\hat{\mathrm{k}}'
\end{aligned} \tag{5}$$

The relations of these vectors are shown as below:

$$\vec{r}_1 + \vec{r}_2 + \vec{r}_3 + \vec{r}_4 = \vec{r}_G \tag{6}$$

From equation (6), two below equations are obtained:

$$\begin{aligned}
y\cos\phi - z\sin\phi &= L + S\cos(\phi+\gamma) - r_c\sin\phi - L\cos\phi \\
y\sin\phi + z\cos\phi + r_c &= S\sin(\phi+\gamma) + r_c\cos\phi - L\sin\phi
\end{aligned} \tag{7}$$

With eliminating S from these two equations, the final equation for second constraint is obtained:

$$\begin{aligned}
z\cos\gamma &= y\sin\gamma - r_c\cos(\gamma+\phi) + L\sin\gamma \\
&+ r_c\cos\gamma - L\sin(\gamma+\phi)
\end{aligned} \tag{8}$$

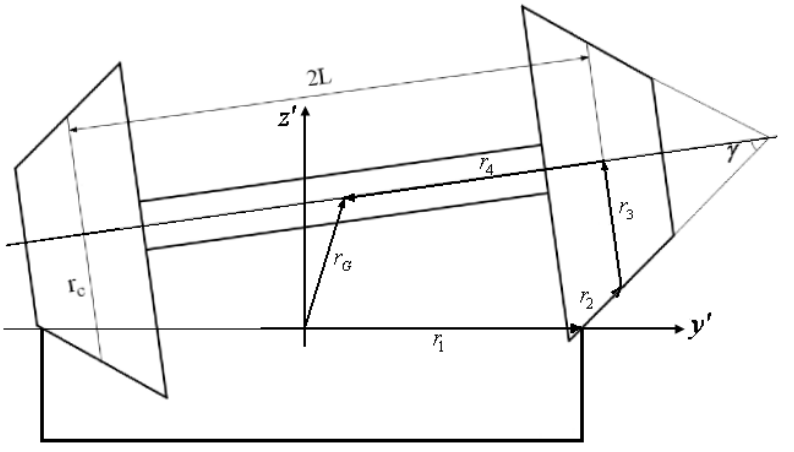

Fig. 4 Relation between r_1, r_2, r_3, r_4 and r_G

Matrices such as T, T', U, and U' are transformation matrices for transforming wheelset coordinate to left contact surface coordinate, wheelset coordinate to right contact surface coordinate, left contact surface coordinate to wheelset coordinate, and right contact surface to wheelset coordinate, respectively. For calculating forces and contact momentums, at first the velocity in contact point should be calculated. For instance the velocity of left side contact point is defined as from relative velocity equation:

$$\vec{V}_{cl} = \vec{V}_G + \vec{\omega} \times \vec{r}_{cl} \tag{9}$$

Where

$$\vec{V}_G = V\hat{I} + \dot{y}\hat{J} + \dot{z}\hat{K} \tag{10}$$

$$\begin{aligned}\vec{V}_{cl} = &\begin{pmatrix} V + \left(\left(\dot{\psi}\sin\phi + \frac{V}{r_c}\right) r_{clz} - \dot{\psi}\cos\phi r_{cly}\right) U_{11} \\ + \left(\dot{y} - \dot{\phi} r_{clz}\right) U_{21} + \left(\dot{z} + \dot{\phi} r_{cly}\right) U_{31} \end{pmatrix} \hat{\mathrm{i}}_{\mathrm{cl}} \\ + &\begin{pmatrix} \left(\left(\dot{\psi}\sin\phi + \frac{V}{r_c}\right) r_{clz} - \dot{\psi}\cos\phi r_{cly}\right) U_{12} \\ + \left(\dot{y} - \dot{\phi} r_{clz}\right) U_{22} + \left(\dot{z} + \dot{\phi} r_{cly}\right) U_{32} \end{pmatrix} \hat{\mathrm{j}}_{\mathrm{cl}} \\ + &\begin{pmatrix} \left(\left(\dot{\psi}\sin\phi + \frac{V}{r_c}\right) r_{clz} - \dot{\psi}\cos\phi r_{cly}\right) U_{13} \\ + \left(\dot{y} - \dot{\phi} r_{clz}\right) U_{23} + \left(\dot{z} + \dot{\phi} r_{cly}\right) U_{33} \end{pmatrix} \hat{\mathrm{k}}_{\mathrm{cl}} \end{aligned} \tag{11}$$

Obtaining the velocity of the right side contact is similar to the left one. Also rotational velocity in the left side contact point is defined as :

$$\begin{aligned}\vec{\omega}_{cl} = &\left(\dot{\phi}\, U_{11} + \left(\dot{\psi}\sin\phi + \frac{V}{r_c}\right) U_{21} + \dot{\psi}\cos\phi U_{31}\right) \hat{\mathrm{i}}_{\mathrm{cl}} \\ + &\left(\dot{\phi} U_{12} + \left(\dot{\psi}\sin\phi + \frac{V}{r_c}\right) U_{22} + \dot{\psi}\cos\phi U_{32}\right) \hat{\mathrm{j}}_{\mathrm{cl}} \\ + &\left(\dot{\phi} U_{13} + \left(\dot{\psi}\sin\phi + \frac{V}{r_c}\right) U_{23} + \dot{\psi}\cos\phi U_{33}\right) \hat{\mathrm{k}}_{\mathrm{cl}} \end{aligned} \tag{12}$$

Then, dynamical creep of the wheelset can be defined as :

$$\begin{aligned} \xi_x &= \frac{V_{cx}}{V} \\ \xi_y &= \frac{V_{cy}}{V} \\ \xi_s &= \frac{\omega_{cz}}{V} \end{aligned} \tag{13}$$

Creep coefficients are constant (f11, f22, f12, f33) and creep forces are obtained as $F'_{cx} = -f_{33}\xi_x$

$$\begin{aligned} F'_{cy} &= -f_{11}\xi_y - f_{12}\xi_{sp} \\ M'_{cz} &= f_{12}\xi_y - f_{22}\xi_{sp} \end{aligned} \tag{14}$$

These forces are hypothesized as limit factors, and the condition of limitation is defined as [6]

$$\beta = \frac{1}{\mu N}\sqrt{F_{cx}'^2 + F_{cy}'^2}$$

$$\varepsilon = \begin{cases} \dfrac{1}{\beta}\left(\beta - \dfrac{\beta^2}{3} + \dfrac{\beta^3}{27}\right) For \beta < 3 \\ \dfrac{1}{\beta} For \beta \geq 3 \end{cases} \quad (15)$$

Also contact forces and momentums are defined as:

$$\begin{aligned} F_{cx} &= \varepsilon F_{cx}' \\ F_{cy} &= \varepsilon F_{cy}' \\ M_{cz} &= \varepsilon M_{cz}' \end{aligned} \quad (16)$$

In this article, the contact force due to nonlinear spring is simulated using a spring with dead band, where the mathematical model is :

$$F_T = \begin{cases} K_T\left(y - \delta\right) & y > \delta \\ 0 & -\delta < y < \delta \\ -K_T\left(y + \delta\right) & y < -\delta \end{cases} \quad (17)$$

In which, K_T is the rail stiffness factor and δ is the clearance of the wheel flange. Figure 5, shows the clearance of the flange as a dead band between the wheel and the rail [4].

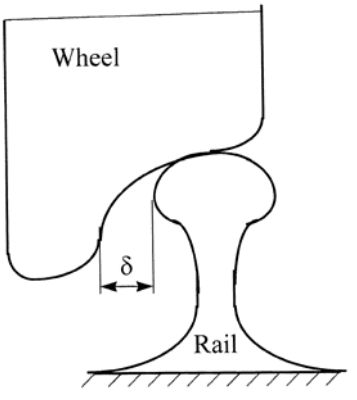

Fig. 5 Clearance and lateral distance between wheel and rail [4]

For suspending in lateral direction, nonlinear suspension has been used that commonly is utilized in freight bogies (Y25). In this condition Kolsch method may be used [7].

$$\begin{aligned} C_0 &= C_h - C_g \\ \dot{K} &= C_0 \dot{y}\left(1 - 0.5\left(sign\left(\dot{y}K\right) + 1\right)\left|\frac{2K}{H}\right|^n\right) \\ F_{sus} &= C_g y + K \end{aligned} \quad (18)$$

According to the modified Euler equations, equations of motion can be written as [8] :

$$\begin{aligned} m\ddot{y} &= F_{clx}T_{12} + F_{cly}T_{22} + F_{crx}T_{12}' + F_{cry}T_{22}' \\ &+ N_{cl}T_{32} + N_{cr}T_{32}' + mg\sin\varphi - F_{sus} - F_T \end{aligned} \quad (19\text{-}1)$$

$$\begin{aligned} m\ddot{z} &= F_{clx}T_{13} + F_{cly}T_{23} + F_{crx}T_{13}' + F_{cry}T_{23}' \\ &+ N_{cl}T_{33} + N_{cr}T_{33}' + mg\cos\varphi \end{aligned} \quad (19\text{-}2)$$

$$\begin{aligned} &I_{xx}\ddot{\varphi} + \dot{\psi}^2\sin\varphi\cos\varphi\left(I_{zz} - I_{yy}\right) - I_{yy}\dot{\psi}\cos\varphi\frac{V}{r_c} = \\ &r_{cly}\left(F_{clx}T_{13} + F_{cly}T_{23}\right) - r_{clz}\left(F_{clx}T_{12} + F_{cly}T_{22}\right) \\ &+ r_{cry}\left(F_{crx}T_{13}' + F_{cry}T_{23}'\right) - r_{crz}\left(F_{crx}T_{12}' + F_{cry}T_{22}'\right) \\ &+ N_{cl}\left(r_{cly}T_{33} - r_{clz}T_{32}\right) + N_{cr}\left(r_{cry}T_{33}' - r_{crz}T_{32}'\right) \\ &+ M_{cl}T_{31} + M_{cr}T_{31}' \end{aligned} \quad (19\text{-}3)$$

$$\begin{aligned} &I_{zz}\left(\ddot{\psi}\cos\varphi - \dot{\psi}\dot{\varphi}\sin\varphi\right) - I_{xx}\dot{\psi}\dot{\varphi}\sin\varphi = \\ &-r_{cly}\left(F_{clx}T_{11} + F_{cly}T_{21}\right) - r_{cry}\left(F_{crx}T_{11}' + F_{cry}T_{21}'\right) \\ &-r_{cly}T_{31}N_{cl} - r_{cry}T_{31}'N_{cr} + M_{cl}T_{33} + M_{cr}T_{33}' \end{aligned} \quad (19\text{-}4)$$

Where:

$$\begin{aligned} r_{clz} &= -(r_c + S\sin\gamma) \\ r_{cly} &= L - S\cos\gamma \\ r_{crz} &= -r_c + S\sin\gamma \\ r_{cry} &= -(L + S\cos\gamma) \end{aligned} \quad (20)$$

3 LATERAL SUSPENSION

For modeling some freight bogies (Y25), a special kind of friction damper has been used. Figure 6, shows the mechanical model of the element [9]. The model contains two springs with stiffness C_0 and C_g, and a dry friction part H. When a displacement is raised in y direction, the first spring C_0, will be deformed until the maximum static friction force in the damper be raised. Before this time, the element works similar to a single spring with stiffness C_h :

$$C_h = C_0 + C_g \quad (21)$$

When the generated force by spring C_0 is more than the maximum static friction force, the frictional part of the element starts to slide and a dynamic friction force is generated opposite to the direction of motion. The total amount of friction force is defined as :

$$F_{friction} = C_g y + K \tag{22}$$

In which

$$\dot{K} = C_0 \dot{y} \left\{ 1 - 0.5\left(1 + sign\left(\dot{y}K\right)\right) \left| \frac{K}{H} \right|^n \right\} \tag{23}$$

Two different models may be considered:

a- The damper force is constant and the maximum amount of H is defined as:

b- $$H = \mu_s \cdot F_{Normal} \tag{24}$$

c- The damper force is not constant, and is force dependent as :

$$H = \mu_s \left(F_{\Pr eload} + C_g x + K \right) \tag{25}$$

In which $F_{\Pr eload}$ is preload frictional force. In this article, the first condition of Kolesch theory is considered.

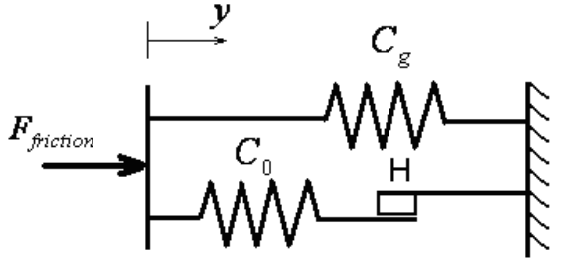

Fig. 6 Mechanical model for Kolesch friction damper

4 SIMULATION AND RESULTS

A wheelset with numerical values as presented in table 1 is considered. Equations (4), (8) and (19) have been solved simultaneously, using Runge-Kuta numerical method. Bifurcation diagram for this dynamical system has been shown in Figure 7. In these conditions critical velocity of wheelset is 33 m/s. Also behavior of wheelset with respect to lateral displacement has been shown in Figure 7.

Table 1 The values of wheelset's constants [4, 6, 7]

m	1800 [kg]
I_{xx}	625.7 [kg.m^2]
I_{zz}	625.7 [kg.m^2]
I_{yy}	133.92 [kg.m^2]
r_c	0.533 [m]
γ	0.05
L	0.7176 [m]
f_{11}	6.728×10^6
f_{12}	1200
f_{22}	1000
f_{33}	6.728×10^6
μ	0.3
g	9.81 [m/s^2]
K_T	1.617×10^8 [N/m]
δ	0.00923 [m]
C_h	2.2×10^6 [N/m]
C_g	4.3×10^5 [N/m]
H	50 [N]
n	2

Figure 8, shows the limit cycle of hunting phenomena. With increasing the velocity, limit cycle will appear. While velocity is smaller than critical velocity, there is no limit cycle and wheelset will return to the equilibrium or central position. Figures 9 and 10 show these behaviors. It should be mentioned that initial displacement was 8 millimeters.

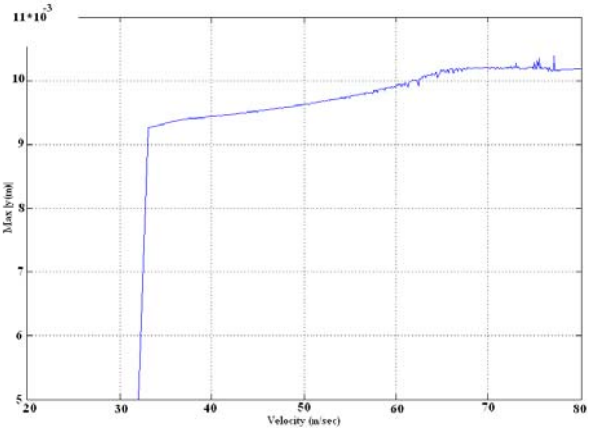

Fig. 7 Bifurcation graph of wheel compared to velocity

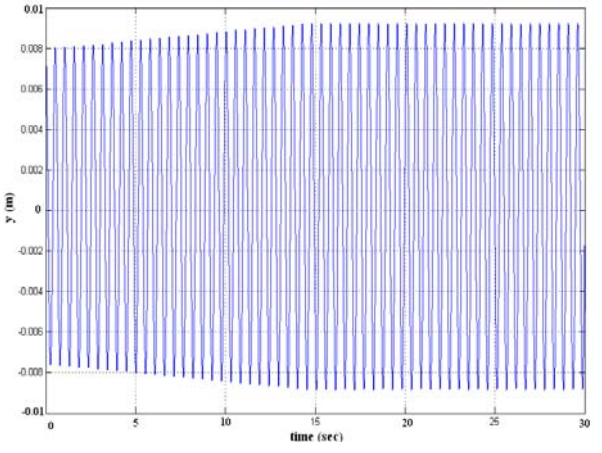

Fig. 8 Lateral displacement graph of wheelset at critical velocity (hunting)

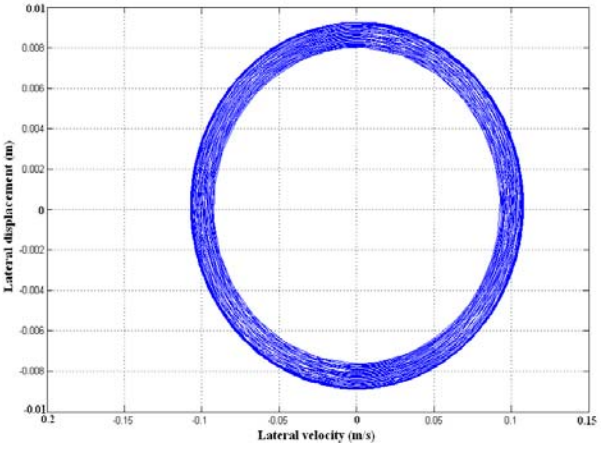

Fig. 9 Limit cycle graph of wheelset at critical velocity (hunting)

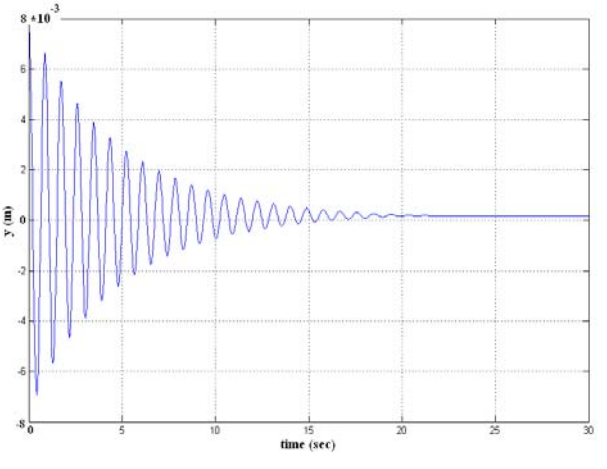

Fig. 10 Lateral displacement graph of wheelset at v=20 m/s

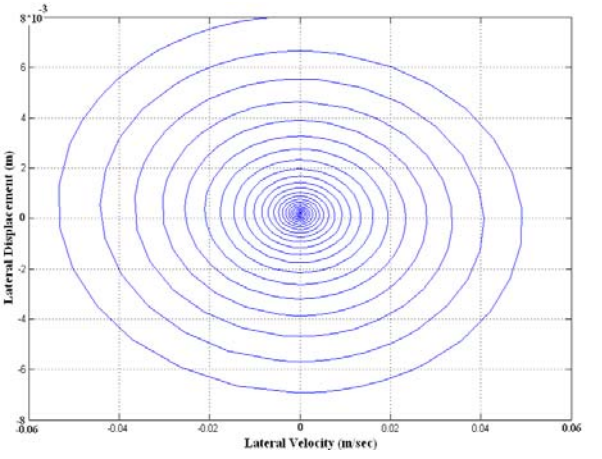

Fig. 11 Limit cycle graph of wheelset at v=20 m/s

5 CONCLUSION

In this paper, nonlinear characteristics of suspension are investigated. While the stiffness of spring C_g =107500 N/m, critical velocity is equal to 15.7 m/s and limit cycle in terms of velocity has been shown in Fig. 12.

Fig. 13 shows critical velocity when C_g =215000 N/m, also Figure 14 shows limit cycle in terms of velocity when C_g =537500 N/m and critical velocity is 36.5 m/s.

Figure 15 shows limit cycle in terms of velocity when C_g =645000 N/m, and critical velocity is 40.1 m/s.

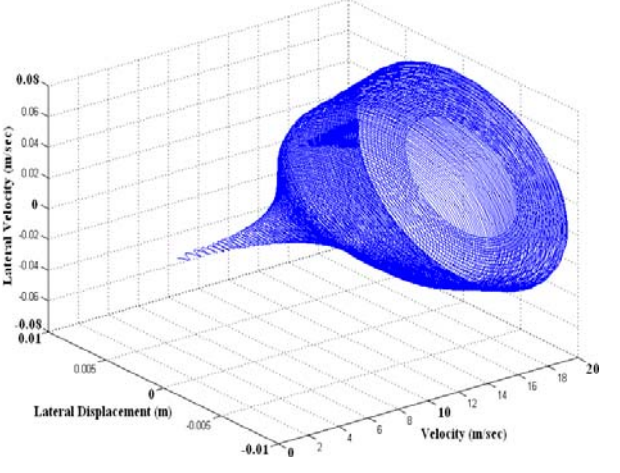

Fig. 12 Limit cycle for C_g =107500 N/m

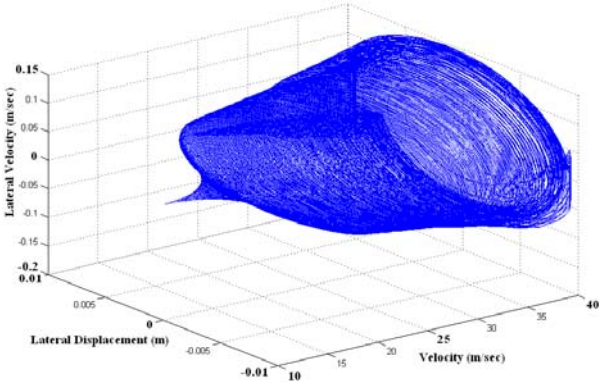

Fig. 13 Limit cycle when C_g =215000 N/m

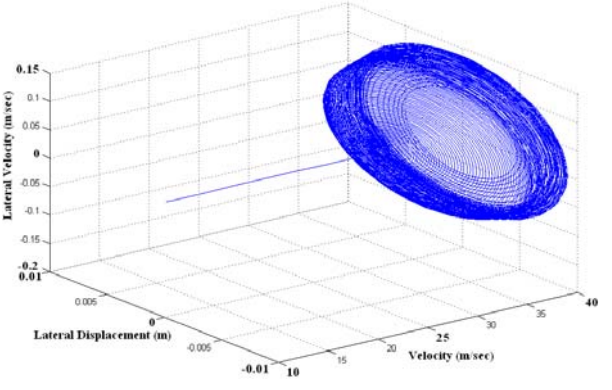

Fig. 14 Limit cycle when C_g =537500 N/m

As the results show, with increasing the C_g, critical velocity is increased. But there is a limitation on the value of C_g. The limitation is the frequency of oscillation of wheelset, because with increasing the stiffness C_g, the frequency of oscillation of wheelset also is increased.

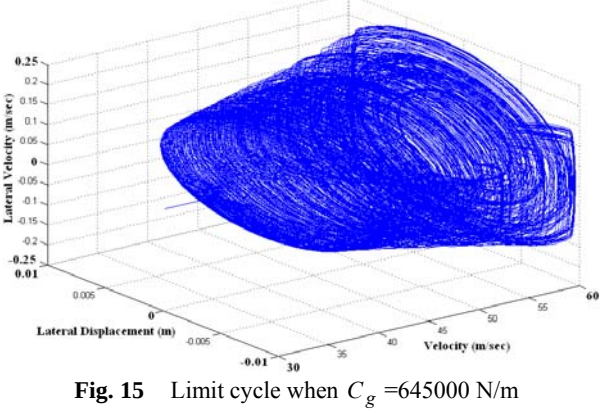

Fig. 15 Limit cycle when C_g =645000 N/m

To analyse the variations of damper forces (*H*), three different cases are considered and critical velocities has been investigated according to Figure 16. *H* depends on kinetic friction coefficient of sliding surfaces of suspension system, weight of the wheelset, and applied load on the axle of the wheelset. Variation of the kinetic friction coefficient is small. Variation of axle load of the wheelset is more affected on value of *H*. Therefore the empty wagon is more critical than the full loaded wagon in view of velocity. Also the effect of *H* is not analogous to the effect of stiffness C_g .

With increasing the values of *H* and C_g, the critical velocity of wheelset will rise, but the effect of *H* on the critical velocity is too small, and the growth of damping force (*H*) will not affect on critical velocity like other parameters of suspension. Therefore, increasing slipping dry friction coefficient or axial load of wheelset will not change the critical velocity as an important dynamical parameter of wheelset. Also when velocity is more than critical velocity, the limit cycle will appear and in this condition, there is an attractor in the system.

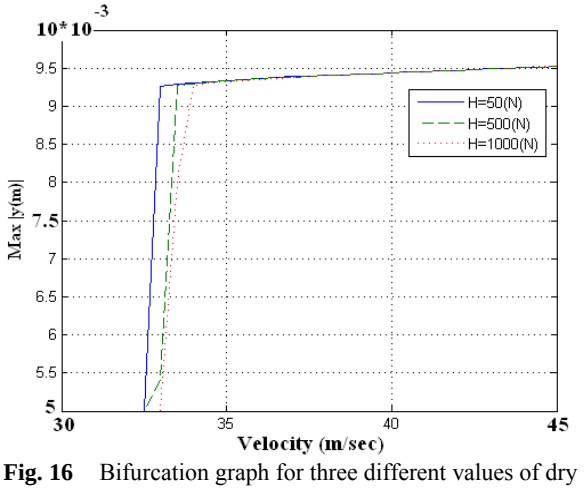

Fig. 16 Bifurcation graph for three different values of dry friction damper force

REFERENCES

[1] Knothe, K., and Böhm, F., "History of stability of railway and road vehicles", Vehicle System Dynamics, 31-1999., pp. 283-323.

[2] Wickens, "The dynamics of railway vehicles - from Stephenson to Carter", Proceedings of the conference From Rocket to Eurostar and beyond, the National Railway Museum London, 5 November 1997.

[3] True, H., and Jensen, C. N., "On a new route to chaos in railway dynamics", Nonlinear Dynamics 13, 1997, pp. 117-129.

[4] Ahmadian, M., and Yang, S., "Hopf bifurcation and hunting behavior in a rail wheelset with flange contac", Nonlinear Dynamics 15, 1998, pp. 15-30.

[5] Yabuno, H., Okamoto, T., and Aoshima, N., "Effect of Lateral Linear Stiffness on Nonlinear Characteristics

of Hunting Motion of a Railway Wheelset", Meccanica 37, 2002, pp. 555-568.

[6] Mohan, A., and Ahmadian, M., "Nonlinear Investigation of the effect of primary suspension on the hunting stability of a rail wheelset", Proceeding of the 2004 ASME/IEEE Joint Rail Conference.

[7] Molatefi, H., Hecht, M., and Kadivar, M. H., "Critical speed and limit cycles in the Y-25 freight wagon", IMechE Vol. 220, Part F: J. Rail and Rapid Transit., 2006.

[8] Baruh, H., "Analytical Dynamics", WBC/McGraw-Hill, 1999.

[9] Lee, S. Y., and Cheng, Y. C., "Hunting stability analysis of high-speed railway vehicles trucks on tangent tracks", Journal of Sound and Vibration, Vol. 282, 2005, pp. 881-898.